

1

AD-A215 611

MULTIMODE SIGNAL PREDICTION ALGORITHM DEVELOPMENT

Radha R. Gupta

THE ANALYTIC SCIENCES CORPORATION
55 Walkers Brook Drive
Reading, Massachusetts 01867



DTIC
ELECTE
DEC 21 1989
S B D

April 1988
TECHNICAL REPORT

Document is available to the U.S. public through the
National Technical Information Service
Springfield, Virginia 22161

Prepared for:

U.S. DEPARTMENT OF TRANSPORTATION
UNITED STATES COAST GUARD
OMEGA Navigation System Center
Alexandria, Virginia 22310

89 12 21 021

| | | | | | |
|---|--|--|--|----------------------------|-----------|
| 1. Report No. | | 2. Government Accession No. | | 3. Recipient's Catalog No. | |
| 4. Title and Subtitle Multimode Signal Prediction Algorithm Development | | | 5. Report Date April 1988 | | |
| | | | 6. Performing Organization Code | | |
| 7. Author(s) Radha R. Gupta | | | 8. Performing Organization Report No. TR-5351-5-1 | | |
| 9. Performing Organization Name and Address The Analytic Sciences Corporation 55 Walkers Brook Drive Reading, MA 01867 | | | 10. Work Unit No. (TRAIS) | | |
| | | | 11. Contract or Grant No. DTCG23-86-C-20024 | | |
| 12. Sponsoring Agency Name and Address U.S. Department of Transportation U.S. Coast Guard Omega Navigation System Center Alexandria, VA 22310 | | | 13. Type of Report and Period Covered Subtask 3 Technical Report | | |
| | | | 14. Sponsoring Agency Code | | |
| 15. Supplementary Notes | | | | | |
| 16. Abstract <p>This report presents a computationally-efficient algorithm based on full-wave waveguide-mode theory for predicting amplitude, phase, and modal interference-induced phase deviation (MIPD) of an Omega station signal for a given location and time. The signal along a path is approximated by a sum of the signal's first few, strongest-amplitude "modes" propagating in the "earth-ionosphere" waveguide formed along the signal path. An inhomogeneous signal path is modeled as a concatenation of a large number of homogeneous segments. For each segment, the algorithm determines the eigenvalue of each of the selected component modes of the multimode signal. The multimode signal propagation across the segment interfaces is determined by connecting the neighboring segment's mode signals using the IPP model's WKB approximation if the mode eigenvalues vary slowly across the interface; otherwise, using the FASTMC model's mode conversion approach. The resulting algorithm provides a reliable and cost-effective prediction of amplitude, phase and MIPD of an Omega station signal for a given location and time.</p> | | | | | |
| 17. Key Words Omega Omega Signal Prediction Model | | | 18. Distribution Statement Document is available to the U.S. Public through the National Technical Information Service, Springfield, Virginia 22161 | | |
| 19. Security Classif. (of this report) Unclassified | | 20. Security Classif. (of this page) Unclassified | | 21. No. of Pages | 22. Price |

NOTICE

This document is disseminated under the sponsorship of the Department of Transportation in the interest of information exchange. The United States Government assumes no liability for its contents or use thereof.

METRIC CONVERSION FACTORS

Approximate Conversions to Metric Measures

| Symbol | When You Know | Multiply by | To Find | Symbol |
|----------------------|----------------------|-------------|--------------------|-----------------|
| LENGTH | | | | |
| in | inches | 2.5 | centimeters | cm |
| ft | feet | 30 | centimeters | cm |
| yd | yards | 0.9 | meters | m |
| mi | miles | 1.6 | kilometers | km |
| AREA | | | | |
| sq in | square inches | 6.5 | square centimeters | cm ² |
| sq ft | square feet | 0.09 | square meters | m ² |
| sq yd | square yards | 0.8 | square meters | m ² |
| sq mi | square miles | 2.6 | square kilometers | km ² |
| acres | acres | 0.4 | hectares | ha |
| MASS (weight) | | | | |
| oz | ounces | 28 | grams | g |
| lb | pounds | 0.45 | kilograms | kg |
| | short tons (2000 lb) | 0.3 | tonnes | t |
| VOLUME | | | | |
| ts | teaspoons | 5 | milliliters | ml |
| fl oz | fluid ounces | 15 | milliliters | ml |
| c | cups | 30 | milliliters | ml |
| pt | pints | 0.24 | liters | l |
| qt | quarts | 0.47 | liters | l |
| gal | gallons | 0.95 | liters | l |
| cu ft | cubic feet | 3.8 | liters | l |
| cu yd | cubic yards | 0.03 | cubic meters | m ³ |
| | | 0.76 | cubic meters | m ³ |

TEMPERATURE (exact)

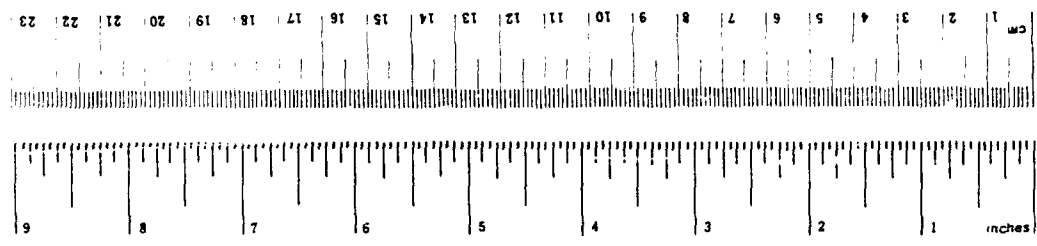
| °F | Fahrenheit temperature | 5/9 (after subtracting 32) | Celsius temperature | °C |
|----|------------------------|----------------------------|---------------------|----|
|----|------------------------|----------------------------|---------------------|----|

Approximate Conversions from Metric Measures

| Symbol | When You Know | Multiply by | To Find | Symbol |
|----------------------------|-----------------------------------|-------------------|------------------------|-----------------|
| LENGTH | | | | |
| mm | millimeters | 0.04 | inches | in |
| cm | centimeters | 0.4 | inches | in |
| m | meters | 3.3 | feet | ft |
| m | meters | 1.1 | yards | yd |
| km | kilometers | 0.6 | miles | mi |
| AREA | | | | |
| cm ² | square centimeters | 0.16 | square inches | in ² |
| m ² | square meters | 1.2 | square yards | yd ² |
| km ² | square kilometers | 0.4 | square miles | mi ² |
| ha | hectares (10,000 m ²) | 2.5 | acres | acres |
| MASS (weight) | | | | |
| g | grams | 0.035 | ounces | oz |
| kg | kilograms | 2.2 | pounds | lb |
| t | tonnes (1000 kg) | 1.1 | short tons | short tons |
| VOLUME | | | | |
| ml | milliliters | 0.03 | fluid ounces | fl oz |
| l | liters | 2.1 | pints | pt |
| l | liters | 1.06 | quarts | qt |
| l | liters | 0.26 | gallons | gal |
| m ³ | cubic meters | 35 | cubic feet | ft ³ |
| m ³ | cubic meters | 1.3 | cubic yards | yd ³ |
| TEMPERATURE (exact) | | | | |
| °C | Celsius temperature | 9/5 (then add 32) | Fahrenheit temperature | °F |

TEMPERATURE (exact)

| °C | Celsius temperature <th>9/5 (then add 32)</th> <th>Fahrenheit temperature</th> <th>°F</th> | 9/5 (then add 32) | Fahrenheit temperature | °F |
|----|--|-------------------|------------------------|----|
|----|--|-------------------|------------------------|----|



© 1993 by The McGraw-Hill Companies. All rights reserved. Printed in the United States of America. ISBN 0-07-051111-1. This book is a trademark of The McGraw-Hill Companies.

TABLE OF CONTENTS

| | <u>Page</u> |
|--|-------------|
| LIST OF FIGURES | iv |
| LIST OF TABLES | v |
| 1. Introduction | 1-1 |
| 2. Omega Signal Propagation | 2-1 |
| 2.1 Signal Propagation Mechanism | 2-1 |
| 2.2 Modal Interference Phenomena | 2-4 |
| 3. Multimode Signal Prediction Algorithm | 3-1 |
| 3.1 Introduction | 3-1 |
| 3.2 Approximations and Assumptions | 3-4 |
| 3.3 Significant Scattering Interface Types | 3-6 |
| 3.4 MSP Algorithm Development | 3-7 |
| 3.4.1 List of Symbols | 3-8 |
| 3.4.2 Algorithm Equations | 3-13 |
| 3.4.3 Signal Amplitude, Phase and MIPD Equations | 3-18 |
| 4. Summary | 4-1 |
| REFERENCES | R-1 |

| | |
|----------------------|-------------------------------------|
| Accession For | |
| NTIS GRA&I | <input checked="" type="checkbox"/> |
| DTIC TAB | <input type="checkbox"/> |
| Unannounced | <input type="checkbox"/> |
| Justification | |
| By _____ | |
| Distribution/ | |
| Availability Codes | |
| Dist | Avail and/or Special |
| A-1 | |

LIST OF FIGURES

| <u>Figure</u> | | <u>Page</u> |
|---------------|---|-------------|
| 2.1-1 | Path-Waveguide Geometry | 2-2 |
| 2.2-1 | An Example of Oscillatory Signal Behavior Caused by Modal Interference in the Signal | 2-5 |
| 2.2-2 | An Example of Modal Interference in the Signal (Mode 2 is Dominant Mode of Signal Beyond 5 Megameters from Transmitter) | 2-5 |
| 2.2-3 | Earth-Ionosphere Waveguide with Day/Night Terminator | 2-7 |
| 3.1-1 | An Illustration of Mode Conversion Phenomenon Occurrence in a Two-Mode Signal (Reflected Modes Are Not Shown) | 3-2 |
| 3.4-1 | N-Segment Path Displaying Mode Conversion/ Scattering at Path-Segment Interfaces Along a N-Segment Long Path | 3-13 |
| 3.4-2 | Multimode Signal E as a Phasor-Sum of E_1 and E_2 (Modes 1 and 2) | 3-19 |

LIST OF TABLES

| <u>Table</u> | | <u>Page</u> |
|--------------|---|-------------|
| 3.2-1 | Day and Night Ionospheric Parameter Values Used In Signal Prediction Algorithm | 3-5 |
| 3 3-1 | Conductivity Grades and Associated Conductivity Levels | 3-8 |

1.

INTRODUCTION

The worldwide navigation position-fixing capability of the Omega Navigation System is predicated on the assumption that the Omega signal, a multimode signal (in the waveguide-mode formulation), can be adequately described by the Mode 1 component* of the signal for any location and time. The lack of Mode 1 dominance in a signal is known as "modal interference". As a consequence of modal interference, the phase of a received Omega signal can deviate (differ) significantly from the modeled phase (which is assumed to be the phase of the Mode 1 component) typically used in computing an Omega position fix. Thus, in a fix computation any use of signal(s) having excessive[†] modal interference-induced phase deviation (MIPD) is expected to degrade the fix accuracy.

The objective of the effort reported herein is to develop a cost-effective algorithm for predicting amplitude, phase, and MIPD of an Omega station signal for a given location and time. This algorithm is required for generating a worldwide database of the amplitude and MIPD of 10.2 and 13.6 kHz Omega system station signals. The database is currently being developed by The Analytic Sciences Corporation (TASC) for the Omega Navigation System Center (ONSC), the U.S. Coast

* Mode 1 is the lowest phase-velocity transverse-magnetic mode of the multimode signal propagating in the "earth-ionosphere" waveguide formed along the signal path (Ref. 1).

† A signal is considered to have excessive MIPD if it exceeds the ONSC-recommended threshold value of 20 centicycles (Ref. 2).

Guard organizational unit which is responsible for operating, maintaining, and improving the Omega system.

An overview of the Omega signal propagation mechanism including modal interference phenomena is given in Chapter 2. The signal prediction algorithm including the assumptions and approximations used to develop the algorithm are presented in Chapter 3. The algorithm development effort is summarized in Chapter 4.

2. OMEGA SIGNAL PROPAGATION

Section 2.1 presents an overview of the Omega signal propagation mechanism. (A detailed discussion of the VLF/Omega propagation theory/mechanism can be found in Refs. 1, and 3 through 8.) A discussion of modal interference phenomena and the resulting signal propagation characteristics is provided in Section 2.2.

2.1 SIGNAL PROPAGATION MECHANISM

Omega signals propagate in the space between the earth's surface and the D-region of the ionosphere, known as the "earth-ionosphere" waveguide (see Fig. 2.1-1). Signal propagation in the waveguide formed along the signal path is conveniently described using a full-wave waveguide-mode representation for the signal. In this representation, a signal is expressed by a sum of the "modes" of the waveguide. Each waveguide mode, a solution of the waveguide-mode equation, is uniquely characterized by its complex eigenvalue. The locally-varying electromagnetic properties* of the signal path determine the propagation characteristics (i.e., amplitude and phase variations) of the signal's component modes and the resulting multimode signal along the path. Signal propagation characteristics of a mode are determined by four locally-varying modal parameters: attenuation rate, phase velocity, excitation factor, and height-gain function. Modal parameters

*Ground conductivity, solar illumination condition, geomagnetic-field magnitude and orientation relative to the signal propagation direction.

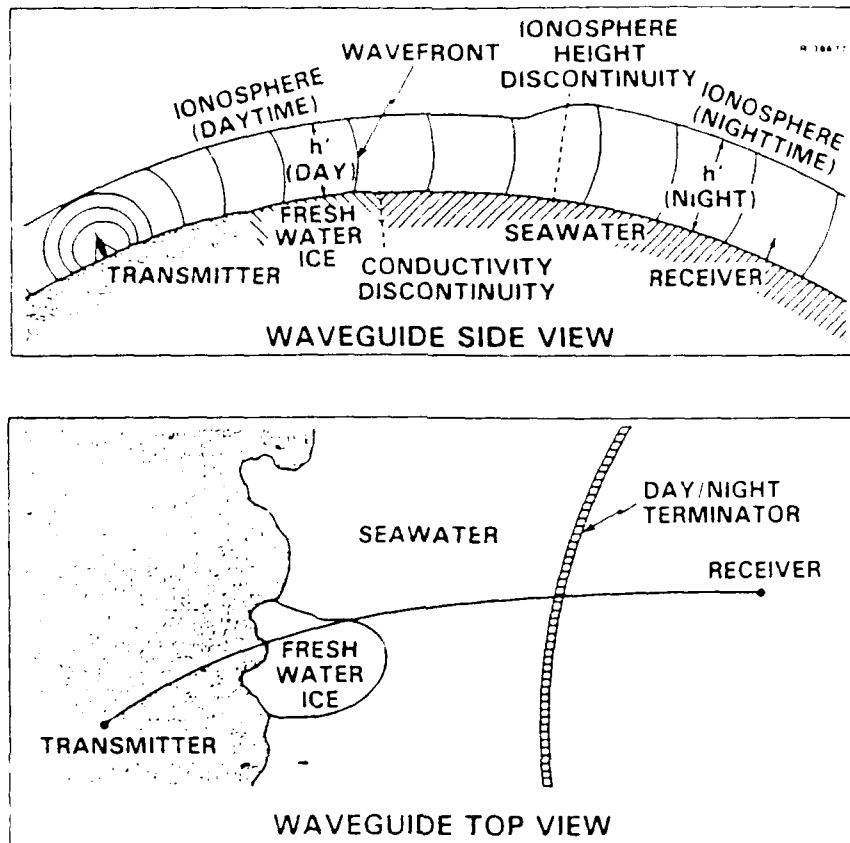


Figure 2.1-1 Path-Waveguide Geometry

depend on the eigenvalue and the electromagnetic properties of the path.

Since an Omega signal path is inhomogeneous due to locally-varying properties of the path, available homogeneous waveguide solution techniques must be modified to include the effects of signal scattering occurring at the path property discontinuities. There are two commonly-used approaches for computing the scattering effects. One uses a mode conversion

* Henceforth in this report the words path, and waveguide are interchangeably used to denote the waveguide formed along the signal path.

approach (Ref. 9); while the other employs a Wenzel-Kramers-Brillouin (WKB)-type approximation (Refs. 1, 8, and 10).

In the mode conversion approach, modes are assumed to be uniquely and independently identifiable in a local sense. Even though the characteristics of a mode depend only on local properties of the path, the propagation of each mode from one point to the next point along a path depends on the local redistribution of the signal energy occurring among its component modes. The redistribution is caused by the mode conversion (see Section 2.3) which occurs at a path point with rapidly-varying mode-eigenvalue(s).

In the WKB-approximation, a mode is assumed to be uniquely and independently identifiable everywhere along a path. Furthermore, each mode is assumed to depend only on local properties of the path and to propagate independently of the existence of any other modes. This approach is applicable to an Ω signal path with gradually-varying mode-eigenvalues. Because scattering effects in the multimode signal have to be computed at each point along a path, a mode conversion-based multimode signal propagation prediction approach is generally much more expensive than a WKB-approximation-based approach.

A cost-effective alternative for determining signal behavior along a path is to use a combination of these two approaches as described in Chapter 3. The next section presents a review of modal interference phenomena.

2.2 MODAL INTERFERENCE PHENOMENA

Although an Omega station signal is, in general, a multimode signal at most locations outside the "near-field*" region of the station, the signal can be adequately approximated by its Mode 1 component. Thus the presence of higher-order modes in the signal can be effectively ignored. Mode 1 is the lowest phase-velocity, transverse-magnetic mode of the signal along the path, and it usually has the lowest signal attenuation rate. The phase of Mode 1 signals, and hence the phase of Mode 1-dominated signals, vary almost linearly with distance from the station.

In the near-field region of a station, as well as along nighttime and transition paths at certain azimuths (especially those paths emanating from the low-geomagnetic-latitude Omega stations), Mode 1 is often not the dominant signal mode (Ref. 10). This lack of Mode 1 dominance is called "modal interference", and the resulting "modally-disturbed" signal is composed of several competing modes which may alternately dominate on different segments of the path. In this case, due to differing phase velocities of the signal's component modes, amplitude/phase of the total (multimode) signal exhibits an oscillatory behavior with distance (see mode-sum signal variations in Fig. 2.2-1). Alternatively, the modally-disturbed signal may be dominated by a single, higher-order mode (e.g., Mode 2 in the signal behavior shown in Fig. 2.2-2) with a linearly-varying phase-versus-distance relationship which is usually significantly different from that of Mode 1.

* A station near-field region typically extends from the station onward to distances of 500-1000 km along "all-day" paths, and 1000-2000 km along "all-night" paths.

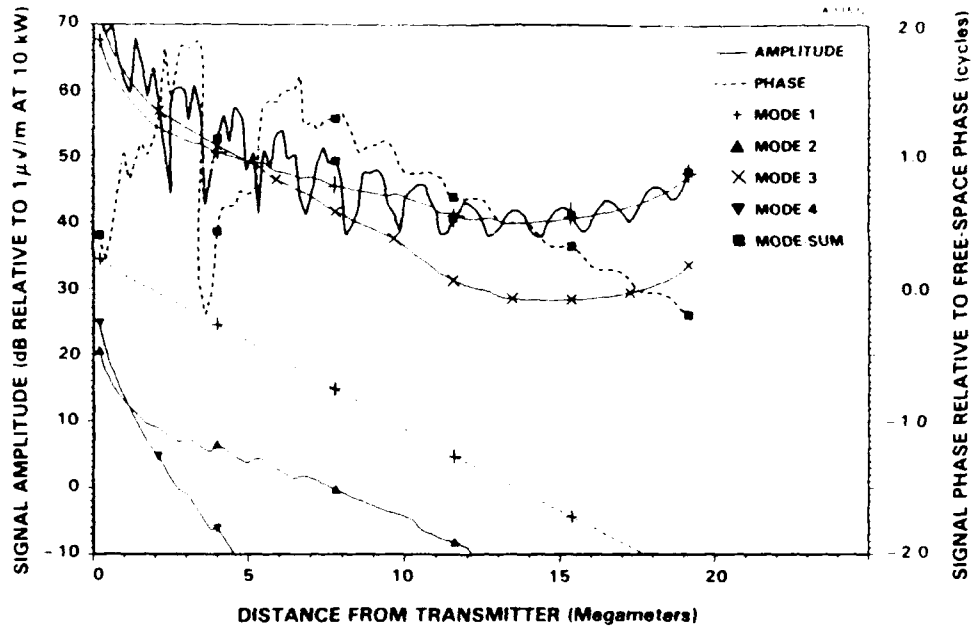


Figure 2.2-1 An Example of Oscillatory Signal Behavior Caused by Modal Interference in the Mode-Sum Signal

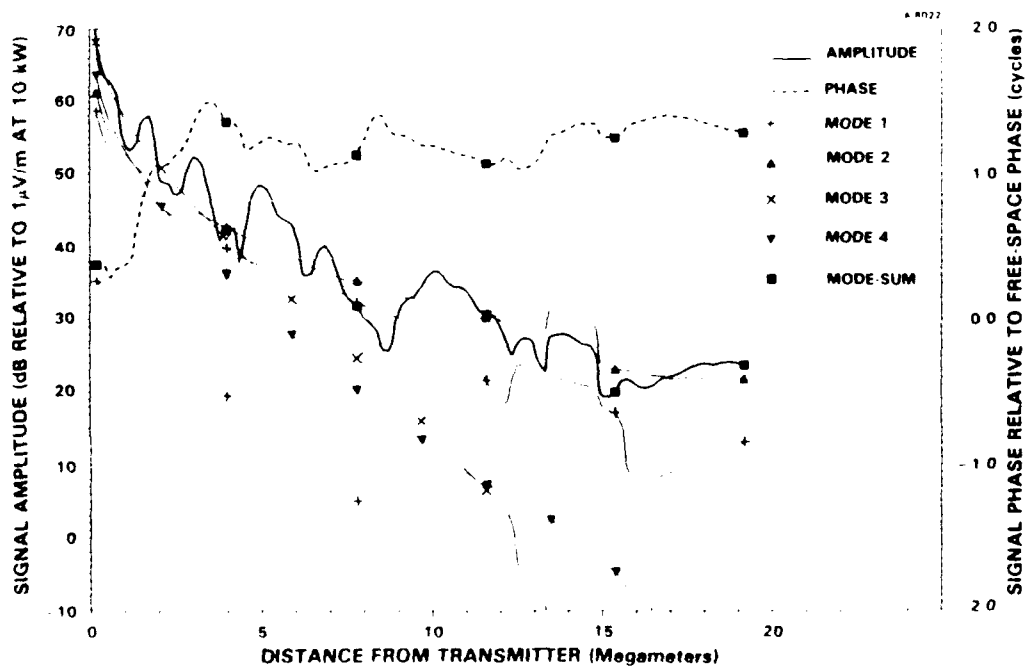


Figure 2.2-2 An Example of Modal Interference in the Signal (Mode 2 is Dominant Mode of Signal Beyond 5 Megameters from Transmitter)

Modal interference in a signal propagating along a path from a transmitting station to a given point is characterized as spatial or temporal, depending upon the solar illumination condition along the path between the station and the point. The interference along a path is classified as spatial interference if the path has an "all-day" or "all-night" illumination condition as the magnitude of interference at each path point is nearly constant in time (and thus depends only on spatial coordinates). If the path is in transition (i.e., the path has a day/night terminator crossing), the interference is referred to as temporal interference. The magnitude of the temporal interference at a point will generally vary in response to the movement of the day/night terminator along the path to the point.

Signal phase deviations arising from spatial interference are generally larger in magnitude and persist to longer distances along a signal path during night than during day. Temporal interference arises from the mode conversion effects occurring at the day/night terminator discontinuity along a transition path (see Fig. 2.2-3) which is subject to the "usual" spatial interference when fully dark. Due to mode conversion, the energy of each incident mode at the path-terminator crossing is converted (or distributed) among several transmitted modes (reflected modes are small at Omega frequencies and are neglected) which propagate beyond the terminator. Thus, because of mode conversion, an Omega station signal with a single dominant mode propagating toward a terminator can exhibit significant modal interference (i.e., presence of several competing modes) in the vicinity of, and beyond the terminator.

G-09125
3-23-88

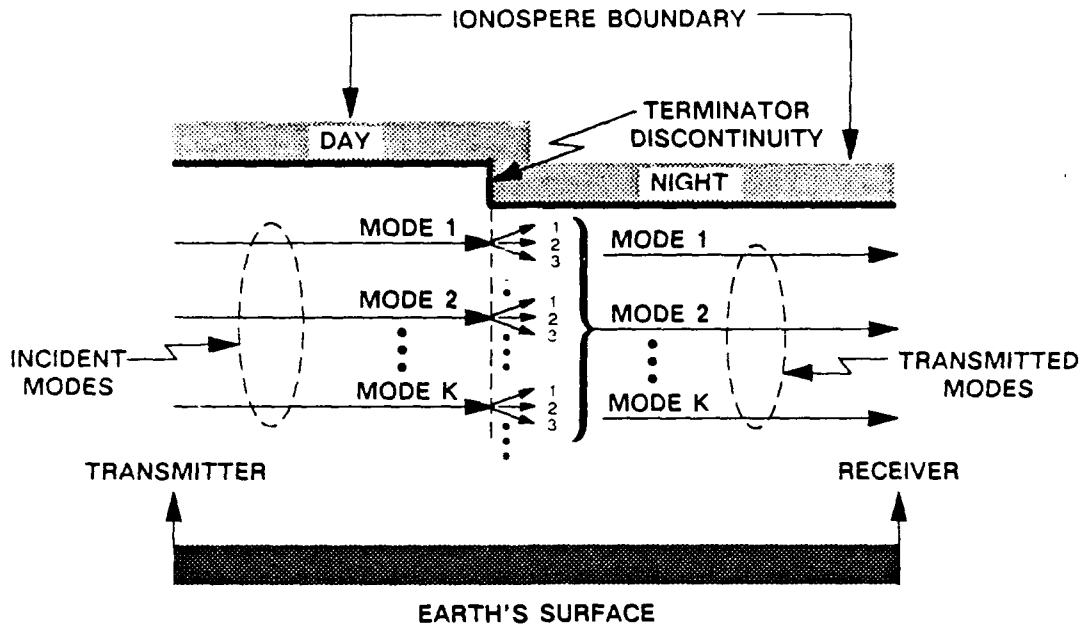


Figure 2.2-3 Earth-Ionosphere Waveguide with Day/Night Terminator

3. MULTIMODE SIGNAL PREDICTION ALGORITHM

3.1 INTRODUCTION

The electric/magnetic field of an Omega signal is a vector quantity composed of three orthogonal field components. Each component is described by a complex quantity with an associated magnitude (amplitude) and phase. The algorithm presented herein is used to generate a worldwide database of the amplitude and MIPD (modal interference-induced phase deviation) of the Omega system station signals. The signal field (also referred herein as simply the signal) of interest for generating the database is the vertical component of the electric field of the signal at the earth's surface. Therefore, subsequent algorithm development is focused on the vertical component of the electric field of the signal.

Since Omega signal paths are inhomogeneous, homogeneous waveguide models cannot be used to determine signal behavior along a path. A commonly-used approximation is to partition the inhomogeneous path into a large number of segments each with constant (electromagnetic) properties associated with the mid-point of the segment. As a consequence of this partitioning scheme, path properties are homogeneous within each segment but change discontinuously at the interface joining the segments. The multimode signal propagation characteristics along the partitioned inhomogeneous path is determined using the following three-step approach. First, multimode signal behavior is obtained along each of the homogeneous segments of the path using a homogeneous waveguide model. Second, the scattering effects in the signal occurring at the

segment interfaces along the path are determined using a mode conversion model or a WKB-approximation. Third, and final, the multimode signal propagation characteristics along each segment are modified to incorporate the scattering effects at the segment interfaces.

A conceptual illustration of the scattering effects due to the mode conversion occurrence at an interface between the neighboring dissimilar property path segments (1) and (2), is shown in Fig. 3.1-1. The incident and transmitted signals are assumed to be composed of Modes 1 and 2, only. In this illustration, E_k^i and E_k^t ($k = 1,2$) are the complex values of the incident (i) and transmitted (t) mode signals associated with k^{th} mode at the interface; $S_{j,k}$ is the complex scattering coefficient which is the ratio of the j^{th} mode of the transmitted signal and k^{th} mode of the incident signal.

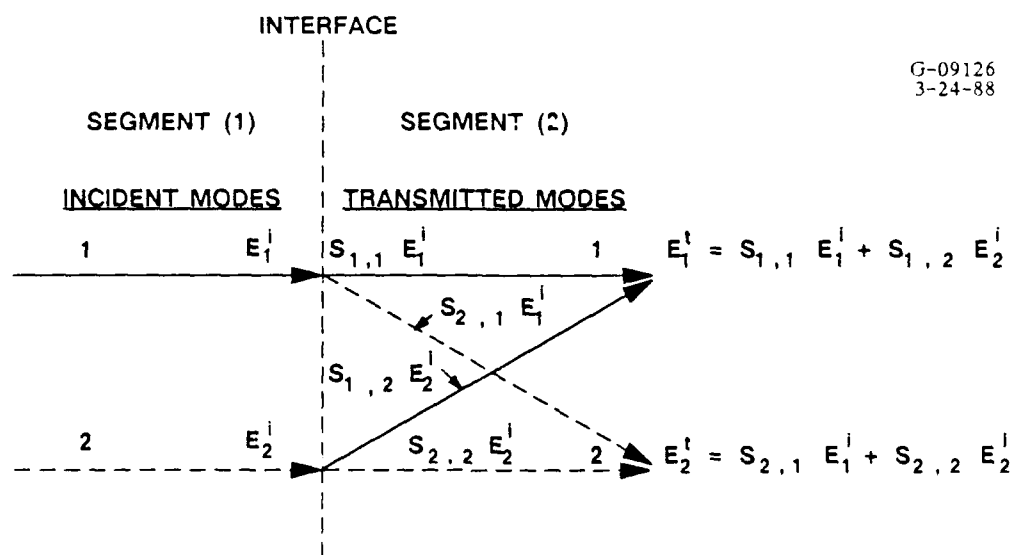


Figure 3.1-1 An Illustration of Mode Conversion Phenomenon Occurrence in a Two-Mode Signal (Reflected Modes Are Not Shown)

This three-step approach for determining multimode signal propagation characteristics along an inhomogeneous signal path is currently implemented in the "Fast Mode Conversion" (FASTMC; Ref. 9) model developed by the Naval Ocean Systems Center (NOSC). Although FASTMC provides reliable signal predictions, it is computationally very expensive.

A cost-effective alternative for computing scattering effects at a path-segment interface with no noticeable loss in the accuracy of the resulting signal is to proceed as follows:

- Identify the expected types of segment interfaces (along worldwide Omega signal paths) where the off-diagonal elements, $S_{j,k}$ ($j \neq k$), of the scattering coefficient matrix are likely to be significant
- Compute scattering effects at a path interface using a mode conversion model, similar to the one implemented in FASTMC (Ref. 9), if the scattering coefficient elements, $S_{j,k}$ ($j \neq k$), at the interface are expected to be significant; otherwise, use a WKB approximation similar to that implemented in the Integrated Propagation Prediction (IPP) model developed by NOSC (Ref. 11).

The Multimode Signal Prediction (MSP) algorithm developed herein is basically the FASTMC model with the provision of computing scattering effects using the WKB-approximation of IPP (instead of FASTMC's mode conversion algorithm) whenever, based on a priori information about the scattering potential of the interface, the off-diagonal scattering coefficient matrix elements are expected to be negligible.

This alternative procedure yields signal predictions within one dB of the FASTMC predictions at about one-tenth of the FASTMC execution time/cost when comparison is made over a representative set of worldwide Omega station signal paths.

The algorithm is designed so that repeated signal calculations along the same path (e.g., at different times of day/year) can be executed for substantially less cost/time than comparable executions of FASTMC. This algorithm will be used to generate a worldwide database of 10.2 and 13.6 kHz signal path calculations for each of the eight Omega stations for 96 times of the year; the total computer cost is projected to be about one percent of the comparable FASTMC cost, which represents a projected savings of several hundred-thousands of dollars to ONSC.

Section 3.2 presents the assumptions and approximations used in development of the MSP algorithm. The list of the path-segment interface types where scattering effects must be computed using the mode conversion model is given in Section 3.3. The MSP algorithm development is presented in Section 3.4.

3.2 APPROXIMATIONS AND ASSUMPTIONS

The MSP algorithm is developed using the following approximations and assumptions concerning the signal path electromagnetic properties, and signal mode structure:

- 1) A day (night) path segment is defined by $0^\circ \leq \chi^* < 90^\circ$ ($90^\circ < \chi \leq 180^\circ$) for all χ along the path segment and a transition segment is one in which $\chi = 90^\circ$ at some point in the segment.
- 2) The day/night ionosphere boundary of the "earth-ionosphere" waveguide (formed along the signal path) is a vertically-stratified, horizontally-homogeneous (in the direction of signal propagation) medium consisting of free electrons (in addition to positive and negative ions) whose day/night density and associated

* χ denotes solar zenith angle.

collision frequency vary exponentially with vertical height (above the earth's surface). Such a day/night ionosphere boundary, in terms of Wait and Spies's notations (Ref. 11), is characterized by a day/night pair of parameters: ionospheric reflection height and ionospheric conductivity gradient. The day/night values of these parameters used in the algorithm are listed in Table 3.2-1.

- 3) The transition, i.e., change from day to night solar illumination condition, along a path is assumed to be a step change in the ionospheric parameters from the day to night values.
- 4) Signal at a day path segment is comprised of the first-three lowest phase-velocity modes, Modes 1 through 3 (Refs. 13 and 14) of the earth-ionosphere waveguide characterizing the path segment.
- 5) Signal at a night path segment is comprised of the first-five lowest phase-velocity modes, Modes 1 through 4 and Mode X (Refs. 12 and 13), of the earth-ionosphere wave-guide characterizing the path segment.
- 6) Mode X's contribution to the multimode signal is negligible along all path segments except for the nighttime, westerly-directed (i.e., geomagnetic bearing* between 190° and 350°) segments in the equatorial (i.e., between 10°N and 10°S geomagnetic latitudes) region, as discussed below.

TABLE 3.2-1
DAY AND NIGHT IONOSPHERIC PARAMETER VALUES USED IN THE MSP ALGORITHM

| IONOSPHERE ILLUMINATION* | IONOSPHERIC PARAMETERS | |
|---------------------------|------------------------------------|---|
| | IONOSPHERIC REFLECTION HEIGHT (km) | IONOSPHERIC CONDUCTIVITY GRADIENT (km ⁻¹) |
| Day (0° ≤ χ < 90°) | 70 | 0.3 |
| Night (90° < χ ≤ 180°) | 87 | 0.5 |
| Transition (χ = 90°) | Step change from 70 to 87 | Step change from 0.3 to 0.5 |

* χ denotes solar zenith angle.

* Geomagnetic bearing is measured clockwise from the geomagnetic north.

In the waveguide-mode theory representation, the odd- and even-numbered modes correspond to the transverse-magnetic (TM) and transverse-electric (TE) modes, respectively, of the earth-ionosphere waveguide. The total signal along a path segment is commonly expressed in terms of the TM and TE modes of the waveguide modeling the path segment. Mode X is a new mode recently identified by TASC and it is found to exist only along a nighttime path and not along a daytime path (Refs. 12 and 13). The dependence of the Mode X eigenvalue and modal parameters on the path properties is significantly different from those of the TM and TE modes. A comparison of the attenuation rate and excitation factor modal parameters of Mode X with those of Modes 1 through 4 has revealed that the contribution of the Mode X signal to the multimode signal is significant (and must be included in the multimode signal calculations) if the path segment is in night and has a westerly geomagnetic bearing, and lies in the equatorial region. This is due to the fact that the "excitability/survivability" of Mode X along a westerly-directed, equatorial path segment is comparable to that of Mode 1. For a path segment that is not westerly-directed and equatorial, attenuation rate of Mode X is 10 to 20 times higher than that of Mode 1; as a consequence, Mode X's contribution to the multimode signal along such a path segment would be insignificant compared to that of Mode 1, and hence can be safely ignored.

3.3 SIGNIFICANT SCATTERING INTERFACE TYPES

This section presents a list of the path-segment interface types where scattering effects must be computed using a mode conversion model. For these interfaces, the eigenvalue(s) of one or more of the component modes of the multimode signal change rapidly across the interface, and thus

cause significant scattering in the signal. The change in eigenvalues at an interface is related to the change in path properties at the interface. The eigenvalue/path-property sensitivity plots (Refs. 12 and 13) can be examined to determine the precise segment-to-segment change in eigenvalues along any portion of a path. This examination has led to identification of the following three interface types where a mode conversion model must be used to compute the scattering effects:

- 1) Interface at the day/night terminator crossing along a path
- 2) Interface in the equatorial region along westerly-directed paths
- 3) Interface with a discontinuity in the path's ground "conductivity grade".

The ground conductivity grades and associated ground conductivity levels are given in Table 3.3-1. In this table, note that conductivity levels 5 through 10 are grouped together and denoted as conductivity grade V because eigenvalues of the signal component modes in this range are insensitive to changes in the conductivity level (Refs. 12 and 13).

3.4 MSP ALGORITHM DEVELOPMENT

This section presents the equations used by the MSP algorithm for computing amplitude, phase, and MIPD of an Omega station signal for a given location and time. The algorithm is based on waveguide-mode theory with: (1) the approximations and assumptions listed in Section 3.2, (2) the significant scattering interface types listed in Section 3.3, and (3) the

TABLE 3.3-1
CONDUCTIVITY GRADES AND ASSOCIATED CONDUCTIVITY LEVELS

| CONDUCTIVITY GRADE | CONDUCTIVITY LEVELS | CONDUCTIVITY VALUE (mho/m) |
|--------------------|---------------------|----------------------------|
| I | 1 | 10^{-5} |
| II | 2 | 3.2×10^{-5} |
| III | 3 | 10^{-4} |
| IV | 4 | 3.2×10^{-4} |
| V | 5 through 10 | 10^{-3} to 4 |

computation of scattering effects outlined earlier in Section 3.1.

Section 3.4.1 gives a list of the symbols used in the algorithm equations. Section 3.4.2 presents the equations for computing the multimode signal along a path. The equations for computing the amplitude, phase, and MIPD of the signal are given in Section 3.4.3.

3.4.1 List of Symbols

This section presents the symbols used in the multimode signal prediction algorithm equations contained in Sections 3.4.2 and 3.4.3.

| <u>Symbol</u> | <u>Definition</u> |
|----------------|---|
| $E(s, r)$ | Vertical component of the multimode signal electric field at path segment s which is at a distance r from the transmitter |
| $E_k(s, r)$ | Vertical component of the k^{th} mode signal electric field at path segment s which is at a distance r from the transmitter |
| $E_k^-(s)$ | Vertical component of the k^{th} mode signal electric field at the point just before the interface between path segments s and $(s+1)$ |
| k, m, n | Mode index subscripts* in path segments 1, 2, 3, respectively |
| m_{N-1}, m_N | Mode index subscripts in path segments $(N-1)$ and N , respectively |
| $M(s)$ | Number of modes included in the multimode signal at path segment s |
| $r(s)$ | Distance from transmitter to the end of path segment s |
| C_0 | Transmitting antenna constant ($= i 2\pi Z I_0 h_0 / \lambda^{3/2}$) |
| Z | Free-space characteristic impedance |
| I_0 | Transmitting antenna current amplitude |

*To avoid clutter in the signal equation, the mode index subscripts k , m , and n are used in place of m_1 , m_2 , and m_3 , respectively.

| <u>Symbol (cont.)</u> | <u>Definition (cont.)</u> |
|----------------------------|---|
| h_0 | Effective height of transmitting antenna |
| λ | Signal wavelength |
| a | Earth's radius |
| i | $\sqrt{-1}$ |
| $\sin^{1/2}(r/a)$ | Geometrical spreading factor describing focusing of signal caused by spherical nature of the earth |
| $\theta_k(s)$ | Eigenvalue (complex quantity) of the k^{th} mode at path segment s |
| K | $\{1-[H/2a]\}$, where H is reference height at which the modified refractive index of the earth-ionosphere waveguide medium is unity |
| $\beta_k(s)$ | $[\gamma_k(s) + i \alpha_k(s)]$, complex value of the propagation constant of the k^{th} mode at path segment s at the earth's surface, as defined in IPP; it is a function of the eigenvalue of the k^{th} mode at path segment s and the path-segment properties |
| $\alpha_k(s), \gamma_k(s)$ | Attenuation rate and phase variation, respectively, of the k^{th} mode at path segment s on the earth's surface, as defined in IPP |
| $ E $ | Amplitude of the complex signal field E |
| ϕ | Phase of the complex signal field E |
| ϕ_1 | Phase of the complex signal field E_1 of Mode 1 signal |
| $\Delta\phi$ | Modal interference-induced phase deviation (MIPD) in the signal |

Symbol (cont.)Definition (cont.)

| | |
|--------------|--|
| $S_{m,k}(p)$ | Scattering coefficient at interface between segment p and segment (p+1) for the k^{th} incident mode and the m^{th} transmitted mode; it is the ratio of the m^{th} transmitted mode signal field and the k^{th} incident mode signal field at the interface; it is computed using either FASTMC's mode conversion model or IPP's WKB-approximation depending upon the interface type (see Section 3.3); under WKB-approximation: $S_{m,k}(p) = \delta_{m,k} [X_k(p+1)/X_k(p)]^{1/2}$, where $\delta_{m,k}$ is unity if $m=k$, and 0.0 otherwise |
| $X_k(s)$ | Excitation factor* (complex value) of the vertical component of electric field of the k^{th} mode at path segment s; it is a measure of relative efficiency with which the k^{th} mode is excited (or received) at path segment s and it is normalized to unity for a segment with infinite ground conductivity along a flat earth |

*Note that the excitation factor definition in the MSP algorithm is slightly different from the definition used in IPP (Refs. 1 and 11). The difference is in the factor: $\sin[\theta_k(s)]$, included in the denominator of the excitation factor equation (see Refs. 1 and 14). IPP uses a $\theta_k(s)$ -value determined at the reference height, H, of 70 km (this is the height where the modified refractive index of the path medium is unity) whereas the MSP algorithm uses a $\theta_k(s)$ -value computed at the earth's surface. Since the signal field of interest is the field at the earth's surface, the IPP-provided excitation factor, $X_k^{\text{IPP}}(s)$, is inappropriate for use in the algorithm, and the correct value is that value used in the algorithm, $X_k(s)$, which is related to the IPP-provided value by the relationship: $X_k(s) = [X_k^{\text{IPP}}(s)] K^{5/2}$, where $K = \{1 - [(H=70)/(2a)]\}$.

Symbol (cont.)

Definition (cont.)

| | |
|----------|---|
| $G_k(s)$ | Height-gain function* (complex value) of the vertical component of the electric field of the k^{th} mode at path segment s , as defined in IPP (Refs. 1 and 11); it gives the variation of the electric field with altitude above the earth's surface and it is normalized to unity at the earth's surface |
|----------|---|

* Note that both the height-gain function, $G_k(s)$ and excitation factor, $X_k(s)$ are defined differently in IPP (Refs. 1 and 11) and FASTMC (Ref. 9). The IPP-defined and FASTMC-defined values are related as:

$$G_k^{\text{IPP}}(s) = -G_k^{\text{FASTMC}}(s) / \sin [\theta_k(s)]$$

$$X_k^{\text{IPP}}(s) = -\sin [\theta_k(s)] X_k^{\text{FASTMC}}(s)$$

$$G_k^{\text{IPP}}(s) X_k^{\text{IPP}}(s) = G_k^{\text{FASTMC}}(s) X_k^{\text{FASTMC}}(s)$$

Since the height-gain function and excitation factor quantities appear as a product in the MSP equation (see Section 3.4.3), either model-provided values for the product can be correctly used in the signal equation.

3.4.2 Algorithm Equations

Signal propagation equations are developed below for a N-segment long path shown in Fig. 3.4-1. Each path segment is characterized by constant (homogeneous) path properties associated with the mid-point of the segment. The multimode signal at segment s is assumed to be composed of $M(s)$ modes. For the sake of clarity in presentation, the MSP algorithm equations for the path shown in Fig. 3.4-1 are presented below: first, along path segment 1; second, along path segment 2; third, along path segment 3; and fourth, along path segment N .

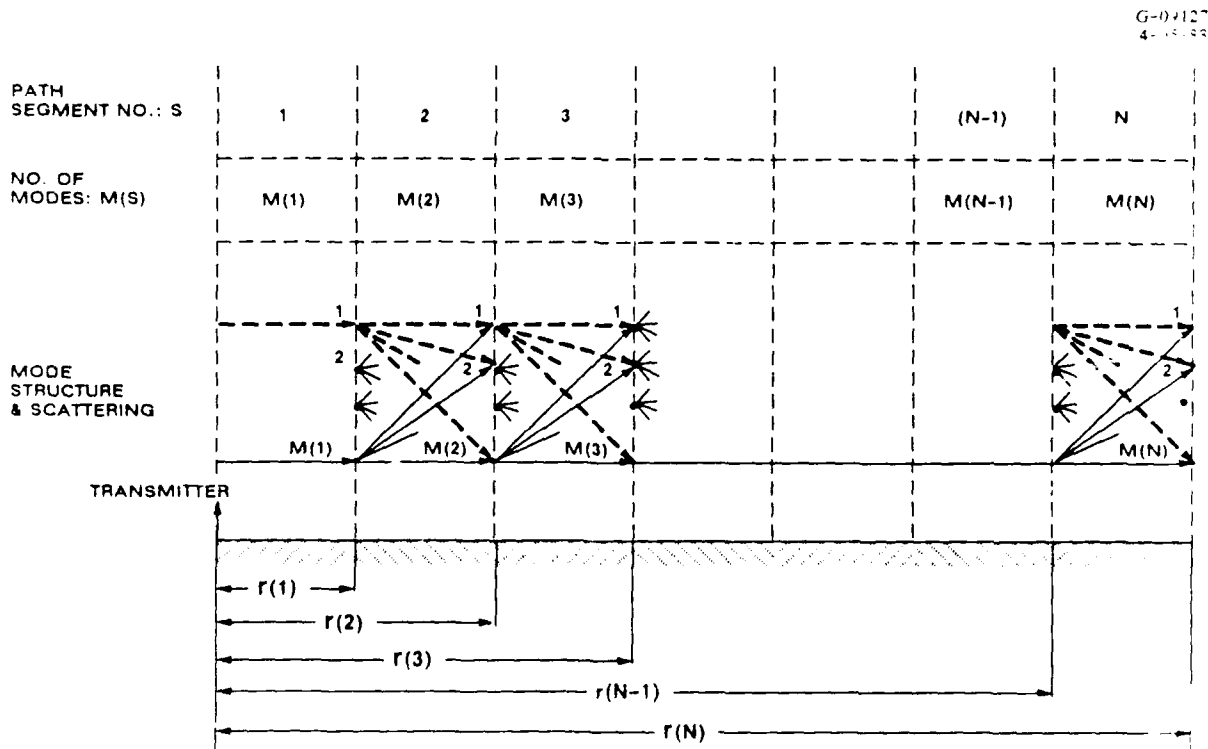


Figure 3.4-1 N-Segment Path Displaying Mode Conversion/Scattering at Path-Segment Interfaces Along a N-Segment Long Path

Note that the excitation factor, $X_k(s)$, in Equation 3.4-1 and elsewhere in this report is the IPP-provided value multiplied by $K^{5/2}$ (see footnotes to the excitation factor and height-gain function definitions presented in Section 3.4.1).

Signal Field Along Path Segment 1

The multimode signal field along path segment 1 (which includes the transmitter but excludes the interface between path segments 1 and 2), at a distance r ($0 \leq r < r(1)$) from the transmitter along the path shown in Fig. 3.4-1, is given by:

$$\begin{aligned}
 E(k,r) &= \sum_{k=1}^{M(1)} E_k(1,r) \\
 &= \underbrace{C_0}_{\text{Freq. \& Trans. Power-Dependent Constant}} \underbrace{\sin^{-1/2}(r/a)}_{\text{Geometric-Spreading Factor}} \sum_{k=1}^{M(1)} \left[\underbrace{\left[\underbrace{X_k(1)}_{\text{Trans.}} \underbrace{X_k(1)}_{\text{Rec.}} \right]}_{\text{Excitation Factors}} \right]^{1/2} \\
 &\quad \times \left[\underbrace{\left[\underbrace{G_k(1)}_{\text{Trans.}} \underbrace{G_k(1)}_{\text{Rec.}} \right]}_{\text{Height-Gain Functions}} \underbrace{\exp \{ i\beta_k(1) [r] \}}_{\text{Propagation Factor of } k^{\text{th}} \text{ mode in Segment 1 over distance } r} \right] \tag{3.4-1}
 \end{aligned}$$

Signal Field Along Path Segment 2

The multimode signal field along path segment 2 (including the interface between path segments 1 and 2 but ex-

cluding the interface between path segments 2 and 3), at a distance r ($r(1) \leq r < r(2)$), from the transmitter along the path shown in Fig. 3.4-1, is given by extending Eq. 3.4-1 as described below:

$$E(2, r) = \sum_{m=1}^{M(2)} E_m(2, r)$$

where

(3.4-2a)

$$E_m(2, r) = \sum_{k=1}^{M(1)} \left[\underbrace{E_k^-(1)}_{\substack{k^{\text{th}} \text{ mode} \\ \text{field just} \\ \text{before} \\ \text{interface} \\ \text{between} \\ \text{Segments} \\ 1 \ \& \ 2}} \right. \underbrace{S_{m,k}(1)}_{\substack{\text{Scatt. coeff.} \\ \text{at interface} \\ \text{between segments} \\ 1 \ \& \ 2 \ \text{describing} \\ \text{conversion of} \\ k^{\text{th}} \ \text{incident} \\ \text{mode signal} \\ \text{into } m^{\text{th}} \ \text{trans-} \\ \text{mitted mode} \\ \text{signal}}} \left. \underbrace{\left[\frac{G_m(2)}{G_k(1)} \right]}_{\substack{\text{Ratio of height-} \\ \text{gain functions} \\ \text{to account for} \\ \text{change in } G \ \text{from} \\ \text{segment 1 to seg-} \\ \text{ment 2}}} \right]$$

$$\times \exp \left\{ \underbrace{i\beta_m(2)[r-r(1)]}_{\substack{\text{Propagation Factor} \\ \text{of } m^{\text{th}} \ \text{mode over} \\ [r-r(1)] \ \text{distance} \\ \text{in Segment 2}}} \right\} \left\{ \underbrace{\sin^{-1/2}[r/a] / \sin^{-1/2}[r(1)/a]}_{\substack{\text{Ratio of Spreading Factors to} \\ \text{account for change in the station} \\ \text{distance from segment 1 to seg-} \\ \text{ment 2}}} \right\}$$

(3.4-2b)

Therefore,

$$E(2, r) = C_o \sin^{-1/2}(r/a) \sum_{m=1}^{M(2)} \sum_{k=1}^{M(1)} \left[X_k(1) G_k(1) \exp \left\{ i\beta_k(1)[r(1)] \right\} \right. \\ \left. \times S_{m,k}(1) G_m(2) \exp \left\{ i\beta_m(2)[r-r(1)] \right\} \right] \quad (3.4-2c)$$

Note that the scattering coefficient $S_{m,k}(1)$ in Eqs. 3.4-2 describes the conversion of the k^{th} incident mode signal

field into the m^{th} transmitted mode signal field due to mode conversion at the interface between path segments 1 and 2. The scattering (or mode conversion) is due to a step change in the path properties at the interface. Also note that for the interface with no discontinuity in the mode-eigenvalue, $S_{m,k}(1) = \delta_{m,k}$, where $\delta_{m,k}$ is Kronecker delta function which is unity for $m=k$ and zero for $m \neq k$. Depending upon the extent of mode-eigenvalue discontinuity at an interface, the scattering coefficients are computed using the FASTMC's mode conversion model (Ref. 9) or IPP's WKB-approximation approach (Ref. 11), as discussed in Sections 3.3 and 3.4.1.

Signal Field in Path Segment 3

The multimode signal field along path segment 3 (including the interface between path segments 2 and 3 but excluding the interface between path segments 3 and 4), at a distance r ($r(2) \leq r < (3)$) from the transmitter along the path shown in Fig. 3.4-1, is given by extending Eqs. 3.4-2 as described below:

$$E(3,r) = \sum_{n=1}^{M(3)} E_n(3,r) \quad (3.4-3a)$$

where

$$E_n(3,r) = \sum_{m=1}^{M(2)} \left[E_m^-(2) S_{n,m}(2) \left[G_n(3)/G_m(3) \right] \right. \\ \left. \times \exp \left\{ i\beta_n(3)[r-r(2)] \right\} \left\{ \sin^{-1/2}[r/a] / \sin^{-1/2}[r(2)/a] \right\} \right] \quad (3.4-3b)$$

Therefore,

$$\begin{aligned}
 E(3,r) = C_o \sin^{-1/2}(r/a) & \sum_{n=1}^{M(3)} \sum_{m=1}^{M(2)} \sum_{k=1}^{M(1)} \left[X_k(1) G_k(1) \right. \\
 & \times \exp\{i\beta_k(1)[r(1)]\} S_{m,k}(1) \exp\{i\beta_m(2)[r(2)-r(1)]\} \\
 & \left. \times S_{n,m}(2) G_n(3) \exp\{i\beta_n(3)[r-r(2)]\} \right] \quad (3.4-3c)
 \end{aligned}$$

Signal Field in Path Segment N

The multimode signal field along path segment N (including the interface between path segments (N-1) and N, but excluding interface between path segments N and (N+1)), at a distance r ($r(N-1) < r < r(N)$) from the transmitter along the path shown in Fig. 3.4-1, is given by extending Eqs. 3.4-3 as described below

$$\begin{aligned}
 E(N,r) = C_o \sin^{-1/2}(r/a) & \sum_{m_N=1}^{M(N)} \dots \sum_{n=1}^{M(3)} \sum_{m=1}^{M(2)} \sum_{k=1}^{M(1)} \left\{ X_k(1) G_k(1) \exp[i\beta_k(1)[r(1)]] \right\} \\
 & \times \left\{ S_{m,k}(1) \exp [i\beta_m(2)[r(2)-r(1)]] \right\} \\
 & \times \left\{ S_{n,m}(2) \exp [i\beta_n(2)[r(3)-r(2)]] \right\} \\
 & \quad \cdot \\
 & \quad \cdot \\
 & \quad \cdot \\
 & \times \left\{ S_{m_N, m_{N-1}}^{(N-1)} G_{m_N}^{(N)} \exp [i\beta_{m_N}^{(N)} [r-r(N-1)]] \right\} \quad (3.4-4)
 \end{aligned}$$

In Eq. 3.4-4, m_N and m_{N-1} denote the mode indices of the component modes of the signal along path segments N and (N-1), respectively; $S_{m_N, m_{N-1}}(N-1)$ is the scattering coefficient at the interface between path segments (N-1) and N for m_{N-1}^{th} incident and m_N^{th} transmitted modes at the interface.

3.4.3 Signal Amplitude, Phase and MIPD Equations

This section develops equations for computing the amplitude, phase, and MIPD (modal interference-induced phase deviation) of the multimode signal from the signal field equations given in Section 3.4.2.

Denoting the in-phase and quadrature components of a signal field by the superscripts i and q, respectively, the amplitude, $|E|$, and phase, ϕ , of the complex signal field, E, are given by:

$$|E| \text{ (Amplitude of E)} = (E_1^2 + E_q^2)^{1/2} \quad (3.4-5a)$$

$$\phi \text{ (Phase of E)} = \tan^{-1}(E^q/E^i) \quad (3.4-5b)$$

Thus, the phase of the Mode 1 component signal field E_1 of the multimode signal E is given by:

$$\phi_1 = \tan^{-1}(E_1^q/E_1^i) \quad (3.4-6)$$

The in-phase and quadrature components of E and E_1 are computed by summing over the component modes:

$$E^i = \sum_{p=1}^P E_p^i = \sum_{p=1}^P E_p \cos \phi_p$$

$$E^q = \sum_{p=1}^P E_p^q = \sum_{p=1}^P E_p \sin \phi_p$$

(3.4-7)

$$E_1^i = E_1 \cos \phi_1 \tag{3.4-8}$$

$$E_1^q = E_1 \sin \phi_1$$

where P is the number of component modes of the multimode signal.

Thus MIPD, $\Delta\phi$, is given by:

$$\Delta\phi = \phi - \phi_1 \tag{3.4-9}$$

Figure 3.4-2 shows MIPD for the case where the multimode signal is composed of two modes (Modes 1 and 2). For the case when the multimode signal is composed of more than two modes (e.g., P modes), Fig. 3.4-2 can be used to determine MIPD by assuming that E_2 is the phasor-sum of Modes 2 through P.

A 5788

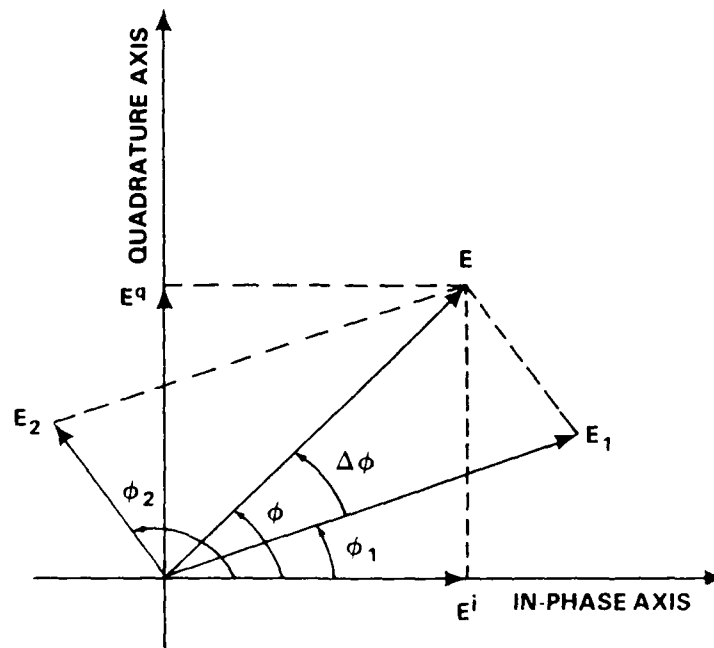


Figure 3.4-2 Multimode Signal E as a Phasor-Sum of E_1 and E_2 (Modes 1 and 2)

4.

SUMMARY

Omega navigation is based on the assumption that an Omega signal, theoretically comprised of an infinite number of modes (in the full-wave waveguide-mode theory representation), is adequately approximated by the signal's Mode 1 component. This is valid at a majority of geographic locations and times. The lack of Mode 1 dominance in a signal is known as "modal interference" and the resulting deviation of the multimode signal phase from the signal's Mode 1 component phase is called modal interference-induced phase deviation (MIPD). Successful use of an Omega navigation signal requires that the signal be strong enough such that its SNR exceeds the receiver detection threshold level and the signal's MIPD be below a certain threshold. The ONSC-recommended value of that threshold is 20 centicycles.

The Analytic Sciences Corporation is developing a worldwide database for the Omega Navigation System Center, consisting of the model-predicted values of the amplitude and MIPD of 10.2 and 13.6 kHz Omega station signals for 96 representative times of the year. The database can be developed from the Naval Ocean System Center's FASTMC computer model (Ref. 9) but this approach is computationally very expensive. The objective of the effort reported herein is to develop a cost-effective Multimode Signal Prediction (MSP) algorithm (based on waveguide-mode theory) for computing the amplitude and MIPD of an Omega station signal for a given location and time.

Since an Omega signal path is inhomogeneous, the algorithm approximates the path as a concatenation of a large number of homogeneous path segments each with constant electromagnetic properties associated with the mid-point of the segment. The signal along a day/night path segment is approximated in the algorithm by the sum of the:

- Three lowest phase-velocity modes (Modes 1 through 3) of the daytime earth-ionosphere waveguide modeling the day path segment
- Five lowest phase-velocity modes (Modes 1 through 4, and Mode X*) of the nighttime earth-ionosphere waveguide modeling the night path segment.

The MSP algorithm consists of:

- (1) Determining modal parameters of the selected component modes of the multimode signal for each of the homogeneous path segments of the signal path; these are conveniently obtained using the TASC-developed look-up table of the multimode signal modal parameters
- (2) Computing scattering effects caused by mode conversion at each of the interfaces (between adjoining path segments) along the signal path using: (a) the FASTMC mode conversion model (Ref. 9) if the eigenvalue of any one of the component modes of the signal varies sufficiently rapidly across the interface, otherwise (b) using the computationally-efficient WKB-approximation used by IPP (Ref. 10)

* Mode X is a new mode recently identified by TASC (Refs. 12 and 13). The propagation characteristics of this mode are comparable to that of Mode 1 along westerly-directed path-segments (with geomagnetic bearings between 190° and 350°, measured clockwise from the geomagnetic north) in the equatorial region (between 10°S and 10°N geomagnetic latitudes). Therefore, Mode X must be included in the multimode signal calculations for these path segments; elsewhere it can be ignored.

- (3) Modifying the individual path-segment multi-mode signal propagation characteristics obtained in step (1) by incorporating the scattering effects computed in step (2) at the segment interfaces.

The resulting MSP algorithm is computationally much more efficient than the FASTMC computer model (Ref. 9). This is because the MSP algorithm computes scattering effects at a path-segment interface using the mode conversion model only if, based on a priori mode-eigenvalue variation information across the interface, the effects are expected to be large; otherwise it uses the WKB-approximation of IPP (Ref. 11). In nearly all cases, the algorithm has been found to provide signal predictions within one dB of the FASTMC predictions at about one tenth of the FASTMC's computer cost.

REFERENCES

1. Gupta, R.R., "Theoretical Background of IPP-2," The Analytic Sciences Corporation, Technical Report TR-343-2, February 1973.
2. Gupta, R.R., Morris, P.B., and Doubt, R.J., "Omega Signal Coverage Prediction Diagrams for 13.6 kHz," Proc. of the Tenth Annual Meeting, International Omega Association (Brighton, England), July 1985.
3. Gupta, R.R., "Omega Navigation System VLF Signal Propagation," The Analytic Sciences Corporation, Technical Report TR-343-2, February 1973.
4. Gupta, R.R., "Mode Interference Studies: Transmitter Excited Interference," The Analytic Sciences Corporation, Technical Report TR-342-10, November 1974.
5. Morris, P.B. and Gupta, R.R., "Omega Navigation Signal Characteristics," Navigation: Journal of the Institute of Navigation, Volume 33, No. 3, Fall 1986.
6. Budden, K.G., Radio Waves in the Ionosphere, Cambridge University Press, London, 1961.
7. Watt, A.D., VLF Radio Engineering, Pergamon Press, Oxford, 1967.
8. Wait, J.R., "Electromagnetic Waves in Stratified Media," Second Edition, Pergamon Press, Oxford, 1970.
9. Ferguson, J.A., and Snyder, F.P., "Approximate VLF/LF Waveguide Mode conversion Model," Naval Ocean Systems Center, NOSC Technical Document 400, November 1980.
10. Donnelly, S.F., "Integrated Propagation Prediction Program Documentation," The Analytic Sciences Corporation, Technical Report TR-343-4, November 1973.
11. Wait, J.R., and Spies, K.P., "Characteristics of the Earth-Ionosphere Waveguide for VLF Radio Waves,"

National Bureau of Standards, NBS Technical Note No. 300, December 1964.

12. Gupta, R.R., "Graphical Display of Omega Signal Modal Parameters, Volume I: 10.2 kHz Signal," The Analytic Sciences Corporation, Engineering Memorandum EM-2650 (Vol. I), September 1987.
13. Gupta, R.R., "Graphical Display of Omega Signal Modal Parameters, Volume II: 13.6 kHz Signal," The Analytic Sciences Corporation, Engineering Memorandum EM-2650 (Vol. II), September 1987.